BIFURCATION OF PLANE-TO-PLANE MAP-GERMS OF CORANK 2

TOSHIKI YOSHIDA, YUTARO KABATA, AND TORU OHMOTO

Dedicated to Professor Masahiko Suzuki on the occasion of his 60th birthday.

ABSTRACT. We describe the bifurcation diagrams of plane-to-plane map-germs of corank two up to $\mathcal{A}_e$-codimension four, and draw some new pictures. Two applications are presented: First, we study the affine differential geometry of crosscaps in 3-space by means of analyzing singularities of projections of the singular surface to the plane. Second, we give some new examples of generic 2-dimensional bifurcations of D_4^+-type planar caustics.

1. INTRODUCTION

1.1. **Sharksfin.** Let us consider the map-germ

$$f : \mathbb{R}^2, 0 \to \mathbb{R}^2, 0, \quad f(x, y) = (x^2 + y^3, y^2 + x^3),$$

whose $\mathcal{A}$-orbit is called the *sharksfin* in Gibson-Hobbs [6] and denoted by $I^{1,1}_{2,2}$ in Rieger-Ruas [18]. Here $\mathcal{A}$ denotes the right-left equivalence in Singularity Theory, i.e., the equivalence of map-germs via actions of diffeomorphism-germs of the source and the target. This is the *least degenerate singularity type of corank two* in $\mathcal{A}$-classification of map-germs, however the structure of nearby $\mathcal{A}$-orbits has not precisely been understood so far; in fact, preceding works [6, 18] missed to detect rigorously the adjacency of swallowtail singularity to the sharksfin. So our first aim of this paper is to analyze the *swallowtail locus* in detail and to present the *true* bifurcation diagram of the sharksfin (Theorem 1.1). Also we will see that the loci of beaks and swallowtail leads us to define a new invariant in the affine geometry of a crosscap in 3-space (Theorem 1.4).

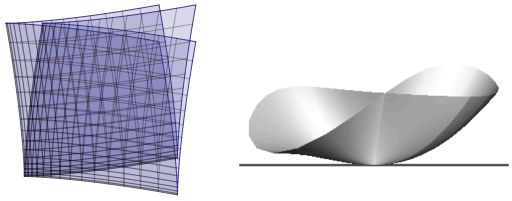

FIGURE 1. Sharksfin and projection of elliptic crosscap

2000 *Mathematics Subject Classification.* 57R45, 53A05, 53A15.

Key words and phrases. $\mathcal{A}$-classification of map-germs, Recognition problem, Singularities of corank two, Bifurcation diagrams, Affine geometry of singular surfaces, Planar caustics.

type	$\mathcal{A}_e$-cod.	normal form
fold	0	(x, y^2)
cusp	0	$(x, y^3 + xy)$
lips	1	$(x, y^3 + x^2y)$
beaks	1	$(x, y^3 - x^2y)$
swallowtail	1	$(x, y^4 + xy)$

TABLE 1. stable and $\mathcal{A}_e$-codimension one mono-germs

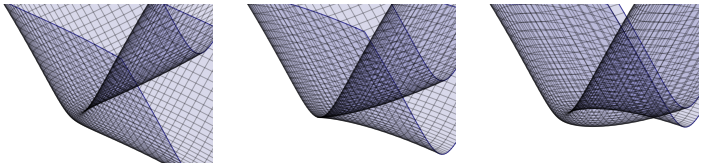

FIGURE 2. Bifurcation of apparent contours (between no.1 and no.3 in Fig.3): It is almost invisible what happens in the middle.

The critical curve of the above germ f has a nodal point at the origin in the source, and its image in the target, called the *apparent contour*, consists of two cuspidal curves meeting at the origin, see Fig.1 (left). This singularity is naturally observed when projecting an *elliptic crosscap* in 3-space to the plane, that was studied in detail by Janet West in her dissertation [21, §5] (For the definition of elliptic, hyperbolic and parabolic crosscaps, see §3.1). Fig.1 (right) suggests two dimensional freedom for perturbing the singular projection, that intuitively means that $\mathcal{A}_e$-codimension of f is equal to two; indeed an $\mathcal{A}$-miniversal unfolding of f is given by

$$F(x, y, a, b) = (x^2 + y^3 + ay, y^2 + x^3 + bx). \tag{1}$$

Take a good representative $F : U \times W \to \mathbb{R}^2$ and define $F_{a,b} : U \to \mathbb{R}^2$ by $F_{a,b}(x, y) := F(x, y, a, b)$. For general $(a, b) \in W$, the map $F_{a,b}$ is C^∞-stable, i.e., it has only singularities of type fold, cusp (Table 1) and double folds (bi-germ). The complementary subset in W is the *bifurcation diagram* $\mathcal{B}_F$, that is the locus where $F_{a,b}$ has *unstable* singularities for some points in U. It consists of several branches corresponding to singularities of $\mathcal{A}_e$-codimension one (i.e., singularities which arise in generic one parameter families of maps):

- local singularity types – *lips, beaks, swallowtail* (Table 1)
- multi-singularity types – *tacnode folds, cusp+fold, triple folds* [13, 6].

Of our particular interest is the local structure of $\mathcal{B}_F$ near the origin.

In an experiment of computer graphics (Fig.2), some qualitative change of apparent contours is observed only when one comes across the axes $a = 0$ and $b = 0$ in the parameter plane – however the process looks unclear (cf. [6, 11]). A natural guess is that this process must be a succession of two local bifurcations of type beaks and swallowtail, that was indeed discussed in Gibson-Hobbs [6]. First we remark that there arise no multi-singularity strata in $\mathcal{B}_F$ [6, §2]. The sharksfin has multiplicity 4, i.e., the maximal number of preimage is 4, thus the bifurcations of type cusp+fold and triple folds do not appear (they have multiplicities 5 and

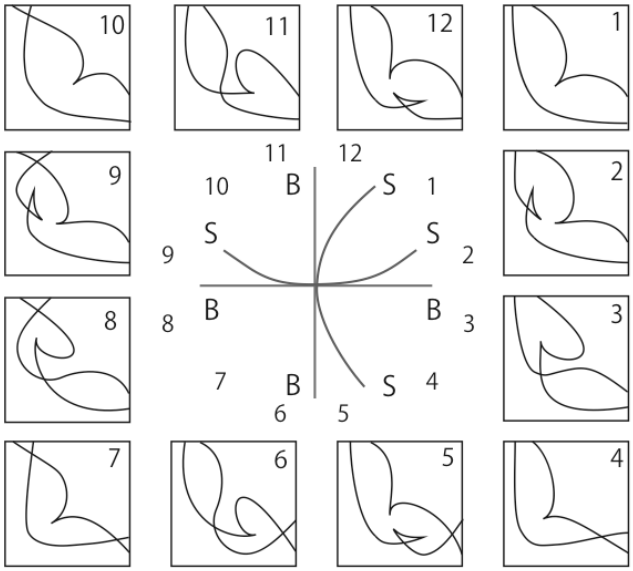

FIGURE 3. Bifurcation diagram in ab-plane consists of the beaks curve B and the swallowtail curve S, and no other local and multi-singularities. The components of B and S have 4-point contact.

6, respectively). The type of tacnode folds has multiplicity 4, but it does not appear, as directly checked: this type arises at distinct two points (x, y) and (X, Y) if $F_{a,b}(x, y) = F_{a,b}(X, Y)$ and the 2×4 matrix

$$[\, dF_{a,b}(x, y)\ dF_{a,b}(X, Y)\,]$$

has rank one; That causes several equations in variables x, y, X, Y, a, b, and it is easily verified that there is no solution (a similar computation will be repeated in §2.3 and §2.4 for more degenerate sharksfin: in these cases we will see that the tacnode appears). Next, as for local singularity types, the lips does not appear, while the beaks appears along the coordinate axes $ab = 0$ [6, 18] (see §2.2). Troublesome is the swallowtail locus: There are three algebraic equations in four variables x, y, a, b, and the task is to eliminate x and y to obtain the desired equation in a and b; However even if one makes use of computer algebra with the software `Singular`, the task turns out to be surprisingly hard, as reported in Gibson-Hobbs [6, p.155]. So there had been no rigorous account about the swallowtail locus as far as the authors know.

Our first result is the following description of the locus together with the picture of apparent contours in Fig.3. It is obtained by an elementary trick and a short computation by hand (§2.2). The theorem is also valid for the complex germ $\mathbb{C}^2, 0 \to \mathbb{C}^2, 0$ of the same form.

Theorem 1.1. *Let F be the $\mathcal{A}$-versal unfolding (1) of the sharksfin $I^{1,1}_{2,2}$. Then the bifurcation diagram $\mathcal{B}_F$ consists of four smooth curve-germs at the origin:*

Beaks: $a = 0$ and $b = 0$
Swallowtail: $a = \frac{1}{16}b^4 + \cdots$ and $b = \frac{1}{16}a^4 + \cdots$

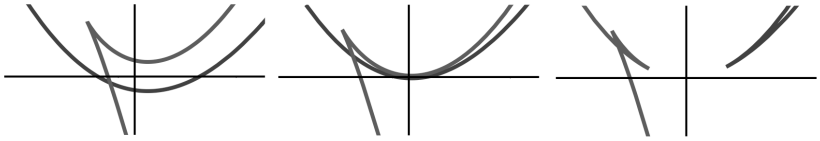

FIGURE 4. Apparent contours (no.4, 3, 2 in Fig.3). Here $a = 0.25$ and $b = -3 \times 10^{-3}$, 0, 3×10^{-5} from the left to the right with the plot ranges $|u| \sim 10^{-3}$ and $|v| \sim 10^{-5}$; the beaks happens at $b = 0$ and the swallowtail happens at $b = \frac{a^4}{16} + \cdots \sim 2.4 \times 10^{-4}$.

Remark 1.2. The fact that the beaks and swallowtail loci have 4-point contact makes these bifurcations *invisible separately* in a naïve experiment of computer graphics (Fig.2). To observe each of those bifurcations solely, we need to find a very particular choice of ranges of variables and a suitable aspect ratio of the graphics as in Fig.4. This is one of typical problems on scaling in the use of computer graphics for the study of singularities, see Morris [11].

1.2. **Deltoid.** The other simplest corank 2 map-germ is given by

$$II^1_{2,2} : \ (x, y) \mapsto (x^2 - y^2 + x^3, xy).$$

This is also of $\mathcal{A}_e$-codimension 2 and naturally arises in parallel projection of a *hyperbolic* crosscap [21, §5]. The bifurcation diagram is known: $\mathcal{B}_F = \{0\}$. Namely, there is no adjacent orbits of $\mathcal{A}_e$-codimension one, and any small perturbation gives a stable maps whose apparent contour is a *deltoid* of fold curve with three cusps (the left of Fig.5). The $\mathcal{A}$-orbits $I^{1,1}_{2,2}$ and $II^1_{2,2}$ are open dense subsets of their $\mathcal{K}$-orbits, $I_{2,2}$ and $II_{2,2}$ defined by $(x^2 \pm y^2, xy)$, respectively.

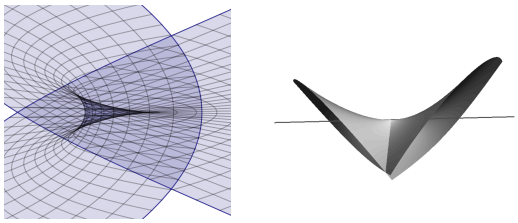

FIGURE 5. Deltoid and projection of hyperbolic crosscap

1.3. **Odd-shaped sharksfin.** In [18] it is shown that a finitely $\mathcal{A}$-determined germ lying on the $\mathcal{K}$-orbits $I_{2,2}$ and $II_{2,2}$ is one of the following types

$$I^{\ell,m}_{2,2} : (x^2 + y^{2\ell+1}, y^2 + x^{2m+1}), \quad II^n_{2,2} : (x^2 - y^2 + x^{2n+1}, xy),$$

with $\mathcal{A}_e$-codimension $\ell + m$ and $2(n+1)$, respectively. They are $\mathcal{A}$-*simple orbits* of corank two, i.e., the cardinality of nearby $\mathcal{A}$-orbits is finite.

The type next to the sharksfin and the deltoid is $I^{2,1}_{2,2}$ of $\mathcal{A}_e$-codimension 3. We call it the *odd-shaped sharksfin* throughout this paper. The apparent contour consists of a 5/2-cusp and a 3/2-cusp meeting at the origin (Fig.6). The miniversal unfolding is given by

$$F(x, y, a, b, c) = (x^2 + y^5 + cy^3 + ay, y^2 + x^3 + bx). \tag{2}$$

type	corank	normal form
butterfly	1	$(x, xy + y^5 + y^7)$
gulls	1	$(x, xy^2 + y^4 + y^5)$
goose	1	$(x, y^3 + x^3y)$
sharksfin	2	$(x^2 + y^3, y^2 + x^3)$
deltoid	2	$(x^2 - y^2 + x^3, xy)$

TABLE 2. mono-germs of $\mathcal{A}_e$-codimension 2.

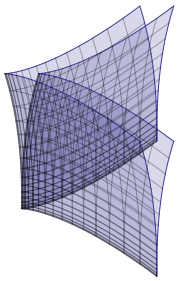

FIGURE 6. Apparent contour of odd-shaped sharksfin

We analyze the bifurcation diagram $\mathcal{B}_F$ in the abc-space. The list of local singularity types of $\mathcal{A}_e$-codimension 2 is seen in Table 2. For multi-singularity types, since $I^{\ell,m}_{2,2}$ has multiplicity 4, it is enough to think only of tacnode folds as mentioned before. The 3D picture of $\mathcal{B}_F$ is drawn in Fig.7: It consists of the following strata:

Sharksfin: the c-axis
Gulls: the b-axis
Beaks: two planes $a = 0$ and $b = 0$
Swallowtail: two smooth surfaces tangent to the beaks locus
Tacnode: half of parabola $4a = c^2$ $(c < 0)$

The abc-parameter space is separated by $\mathcal{B}_F$ into thirteen open connected domains corresponding to different types of stable maps $F_{a,b,c}$. A generic two-dimensional section of $\mathcal{B}_F$ passing through the origin is depicted in Fig.8; when deforming the section, the odd-shaped sharksfin breaks into two isolated singularities of type sharksfin and gulls. This section meets nine open domains among thirteen ones, and corresponding apparent contours are viewed in Fig.9. Compare Fig.9 with the previous Fig.3 for sharksfin; the tacnode curve appears, the apparent contours indexed by no. 11 and 12 are changed, and a smooth component of swallowtail has at least 7-point contact with a component of beaks.

For more degenerate sharksfin of type $I^{2,2}_{2,2}$, the bifurcation diagram is placed in parameter 4-space, and its generic hyperplane section can be depicted in a similar way as Fig.7, see §2.4. On one hand the bifurcation diagram of $II^2_{2,2}$ is formed only by the deltoid $II^1_{2,2}$ and there is no branch corresponding to singularity type of corank one.

A generic 3-parameter family may meet the singularity type $I_{2,3} : (x^2, y^3)$, but it is not $\mathcal{A}$-simple: Indeed the $\mathcal{K}$-orbit $I_{2,3}$ is formed by a family of $\mathcal{A}$-orbits with

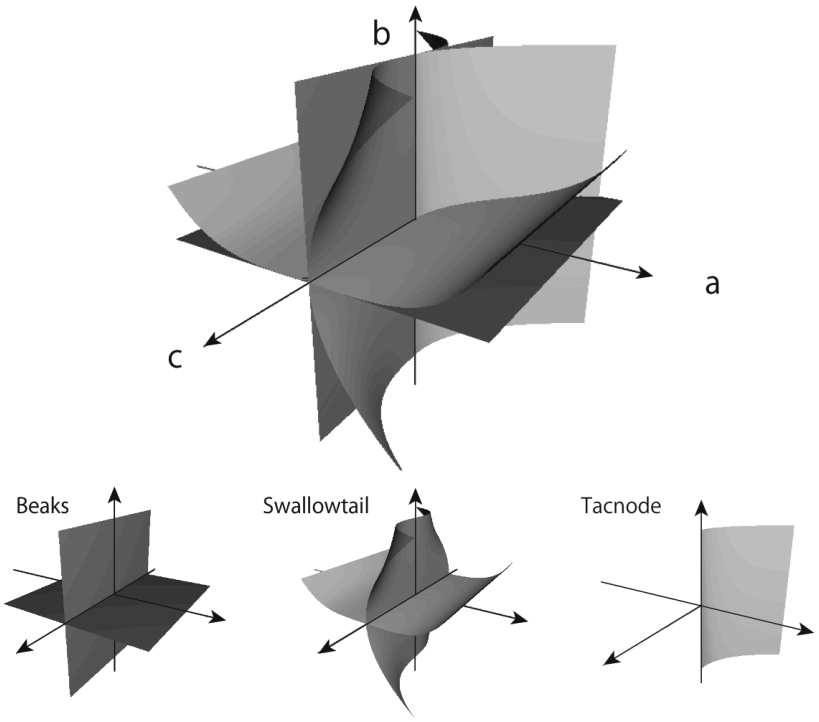

FIGURE 7. Bifurcation diagram of the odd-shaped sharkskin

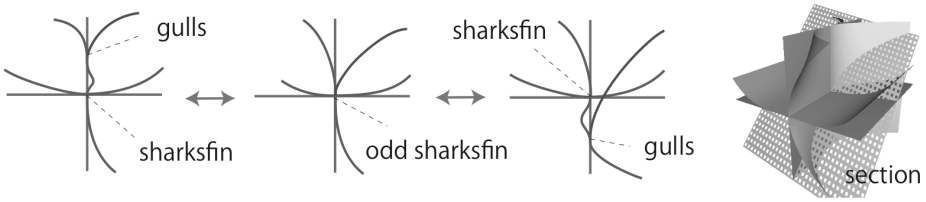

FIGURE 8. Generic section of the bifurcation diagram in Fig.7.

the modality greater than one [18, Lem.2.3.3]. We will deal with the bifurcation of this type in another paper [23].

1.4. **Central projection of crosscaps.** The first application is about the flat or affine differential geometry of singular surfaces with crosscaps in 3-space in relation with central projections from arbitrary viewpoints, that generalizes the study on singularities of projections of smooth surfaces [1, 2, 3, 4, 7, 9, 16, 20, 21].

A *parallel projection* of a smooth surface $M \subset \mathbb{R}^3$ means the restriction to M of a linear orthogonal projection $\mathbb{R}^3 \to \mathbb{R}^2$. When varying the kernel direction of projections in a small open set $U \subset \mathbb{R}P^2$, we have a 2-parameter family of maps $M \times U \to \mathbb{R}^2$. Arnold [1] and Bruce [4] classified singularities arising in parallel projections of a generic smooth surface; the obtained list coincides with the list of corank one germs of $\mathcal{A}_e$-codimension ≤ 2 given in Tables 1, 2. As a generalization,

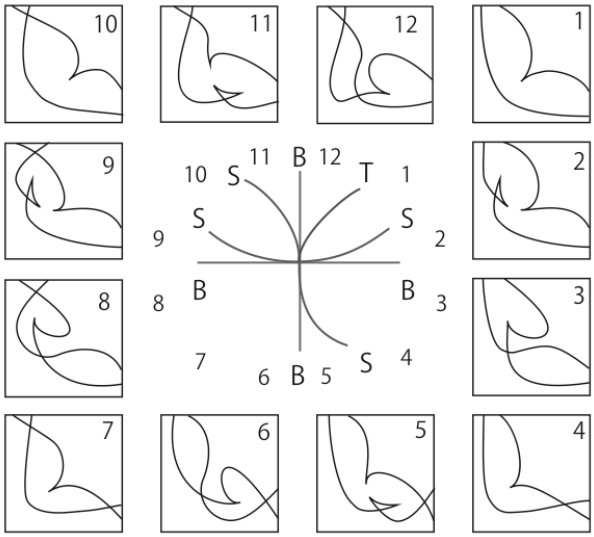

FIGURE 9. The bifurcation diagram associated to the section in Fig.8: It consists of the beaks curve B, the swallowtail curve S and the tacnode curve T.

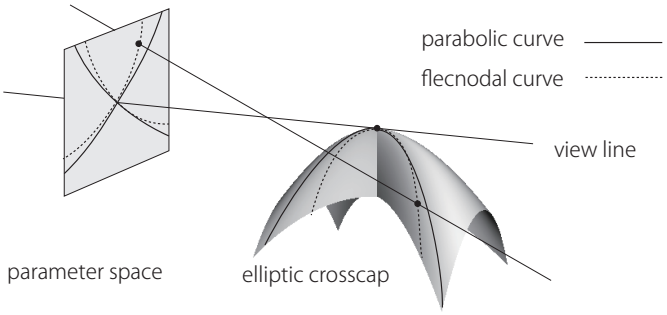

FIGURE 10. A generic elliptic crosscap and view lines of central projections.

West [21] considered singularities of the parallel projection of a singular surface with crosscap: it is proved that when viewing the crosscap along its image tangent line, the sharksfin and the deltoid occur in general.

A *central projection* of M from a *viewpoint* $p \in \mathbb{R}^3 - M$ is the restriction to M of the natural projection

$$\pi_p : \mathbb{R}^3 - \{p\} \to \mathbb{R}P^2, \quad \pi_p(x) := \text{the line generated by } x - p.$$

When varying viewpoints p in a small open set $U \subset \mathbb{R}^3 - M$, we have a 3-parameter family $\varphi : M \times U \to \mathbb{R}^2$. In Platonova [16] (Shcherbak, Goryunov [7, 1]), singularities arising in such a family φ for generic smooth surfaces are classified: the obtained list of singularities slightly differs from the list of $\mathcal{A}$-classification of map-germs – some germs of $\mathcal{A}_e$-codimension 3 do not appear in central projection of generic

surfaces. That means that this geometric setting puts a rather strong restriction on the appearance of singularities of map-germs (see also Kabata [9]).

The same thing happens for corank 2 singularities. We extend West's result to the case of central projection of crosscaps as follows:

Theorem 1.3. *For a generic crosscap at $x_0 \in M$ of a smooth map $\iota : M \to \mathbb{R}^3$, it holds that for arbitrary point p_0 lying on the image line of $d\iota(x_0)$ in the ambient space $\mathbb{R}^3$, the germ at x_0 of the central projection $\pi_{p_0} \circ \iota : M \to \mathbb{R}P^2$ is $\mathcal{A}$-equivalent to either of sharksfin or deltoid.*

The proof will be given in §3.1. Note that it is not quite obvious that the odd-shaped sharksfin does not appear in general, that is the main point of the above theorem. Also the singularity type of $I_{2,3}$ does not appear, although it has codimension 5 in $J(2,2)$. This case is obvious: indeed a singularity of type $I_{2,3}$ occurs in projections when one views a *parabolic* crosscap, but it is not generic in the space of map-germs with crosscaps.

Differential geometry of crosscaps has been studied by several authors, e.g., [21, 5, 8, 20, 15], while the counterpart in affine differential geometry has been less taken attention. A common particular feature is the *parabolic curve*: It is defined by the closure of regular points on the surface where the Gaussian curvature vanishes, in other words, it is the locus on the surface where the parallel projection along the asymptotic line has the beak/lips singularity (or more degenerate singularity). It is shown in West [21] that the parabolic curve does not approach to a hyperbolic crosscap point, while there are two smooth components of the curve passing through an elliptic crosscap point. Another important characteristic in affine differential geometry is the *flecnodal curves* or the *curve of inflections of asymptotic lines* [1, 16]. The curve consists of regular points of the surface so that an asymptotic line at that point has (at least) 4-point contact with the surface, that is also characterized by the vanishing of the so-called Pick invariant. In other words, it is the locus on the surface where the swallowtail (or more degenerate) singularity occurs in the parallel projections along the asymptotic lines. As a byproduct of Theorem 1.1, we show the existence of the flecnodal curve near an elliptic crosscap, like as the parabolic curve just as mentioned. In fact, the *order of contact of these two curves* is a new invariant which exactly characterizes *generic* elliptic crosscaps in Theorem 1.3.

Theorem 1.4. *The flecnodal curve approaches to any elliptic crosscap; it has two smooth components passing through the crosscap point. In the source space parametrizing the crosscap at $x_0 \in M$, each component of the flecnodal curve is tangent to a component of the parabolic curve at x_0 with odd contact order; in particular, both pairs of components of these curves have 3-point contact if and only if the crosscap is generic in the sense of Theorem 1.3, i.e., the projection of the crosscap along the image tangent line is of type sharksfin. The flecnodal curve does not approach to any hyperbolic crosscap.*

1.5. **Planar caustics.** We present another application of our bifurcation diagrams of (degenerate) sharksfin.

A special class of plane-to-plane maps is given by *Lagrange maps*, in other words, *gradient maps* $(\frac{\partial h}{\partial x}, \frac{\partial h}{\partial y})$ of functions $h(x, y)$ on the plane. The critical value set of a Lagrange map is called a *planar caustics*.

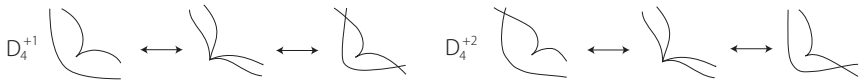

FIGURE 11. D_4^+-perestroika of planar caustics.

For studying the diffeomorphic types of caustics, there is the *caustics-equivalence* of Lagrange maps, that is just the $\mathcal{A}$-equivalence as ordinary maps (i.e., we forget the factorization via Lagrange immersions and projection of the cotangent bundle). As known, generic singularities of planar Lagrange maps are the same as stable singularities of plane-to-plane maps, while non-generic case are completely different. For instance, the *D_4^+-perestroika* due to Arnold-Zakalyukin [2, 3, 24], depicted in Fig.11, is a generic one-parameter family of planar caustics, but not generic as a family of ordinary maps; indeed the family is induced from the versal unfolding of sharksfin such as $F(x, y, a(t), b(t))$, where F is of the form (1) and $(a(t), b(t))$ is a non-singular curve-germ at the origin which is transverse to both a and b-axes, i.e., path through the origin joining no.1 and no.7, or no.4 and no.10, in Fig.3 (see also §4.2.1).

There has been almost nothing known about generic 2-dimensional bifurcations of planar caustics (cf. [14]). It would therefore be meaningful to seek for some 2-dimensional families of Lagrange maps embedded in a higher dimensional versal unfolding of degenerate sharksfin, as an analogy to the relation between the D_4^+-perestroika and the sharksfin. In this heuristic way, we find some new examples of 2-dimensional bifurcations of planar D_4^+-caustics in §4.

Note: This article is part of master-course theses of the first and second authors in Hokkaido university [9, 22]. The authors thank Kentaro Saji for his interests, Farid Tari for making our attention to Janet West's thesis, and the referee for comments suggesting to improve the 1st draft. This work is partly supported by the JSPS grant no.23654028.

2. Bifurcation Diagrams

2.1. **Recognition of $\mathcal{A}$-types of corank one.** For the $\mathcal{A}$-classification of plane-to-plane germs, see [1, 7, 17, 18]. Recall that $f, g : \mathbb{R}^2, 0 \to \mathbb{R}^2, 0$ are *$\mathcal{A}$-equivalent* if there is a pair (σ, τ) of diffeomorphism germs of source and targets at the origins so that $g = \tau \circ f \circ \sigma^{-1}$. The corank of f means $\dim \ker df(0)$. The $\mathcal{A}_e$-codimension of f is just the minimum number of parameters required for constructing $\mathcal{A}$-versal unfolding of f; in particular, f is a stable germ if and only if its $\mathcal{A}_e$-codimension is 0.

The normal forms of plane-to-plane germs with $\mathcal{A}_e$-codimension ≤ 2 are listed in Tables 1 and 2. Given a map-germ, a natural question is to ask which $\mathcal{A}$-type in the list the germ belongs to, that is often referred to as a *recognition problem of map-germs*. An elementary *coordinate-free* approach to this problem is introduced by Saji [19] and Kabata [9] (for fold and cusp, it is essentially due to H. Whitney): Given a map-germ $f = (f_1, f_2) : \mathbb{R}^2, 0 \to \mathbb{R}^2, 0$ of corank one, let us take

- the Jacobian $\lambda(x, y) := \frac{\partial(f_1, f_2)}{\partial(x, y)}$

(fold)	$\eta\lambda(0) \neq 0$
(cusp)	$d\lambda(0) \neq 0$, $\eta\lambda(0) = 0$, $\eta^2\lambda(0) \neq 0$
(swallowtail)	$d\lambda(0) \neq 0$, $\eta\lambda(0) = \eta^2\lambda(0) = 0$, $\eta^3\lambda(0) \neq 0$
(lips)	$d\lambda(0) = 0$, $\det \mathrm{H}_\lambda(0) > 0$
(beaks)	$d\lambda(0) = 0$, $\det \mathrm{H}_\lambda(0) < 0$, $\eta^2\lambda(0) \neq 0$
(butterfly)	$d\lambda(0) \neq 0$, $\eta\lambda(0) = \eta^2\lambda(0) = \eta^3\lambda(0) = 0$, $\eta^4\lambda(0) \neq 0$
(gulls)	$d\lambda(0) = 0$, $\det \mathrm{H}_\lambda(0) < 0$, $\eta^2\lambda(0) = 0, \eta^3\lambda(0) \neq 0$
(goose)	$d\lambda(0) = 0$, $\mathrm{rk}\, \mathrm{H}_\lambda(0) = 1$, $\eta^2\lambda(0) \neq 0, \theta^3\lambda(0) \neq 0$.

TABLE 3. Criteria (of jets) of $\mathcal{A}$-orbits of corank one germs.

- any vector field η near the origin so that $\eta|_{\lambda=0}$ spans $\ker df$.

We put $\eta^k\lambda = \eta(\eta^{k-1}(\lambda))$. Denote $d\lambda = \frac{\partial\lambda}{\partial x}dx + \frac{\partial\lambda}{\partial y}dy$, the differential of λ. Additionally, if the Hessian matrix H_λ of λ at 0 has rank one, let θ be a vector field so that $\theta(0)$ spans $\ker \mathrm{H}_\lambda(0)$. Then a geometric characterization of $\mathcal{A}$-types in Tables 1, 2 is described as in Table 3 [19, 9]. The criteria for lisps, beaks and swallowtail have been given in [19], and it is not difficult to see that the same argument also leads to the above conditions for butterfly, gulls and goose: In fact, the normal form of each $\mathcal{A}$-type satisfies the corresponding condition; Conversely, given a corank one germ $(x, g(x, y))$, take $\eta = \frac{\partial}{\partial y}$, then each condition in Table 3 fixes the jet of g to be of a particular form. The key is the following lemma:

Lemma 2.1 ([19, 9])**.** *The conditions on λ, η and θ in Table 3 are independent from the choice of coordinates of the source and target and the choice of η and θ.*

Precisely saying, for instance, the above condition for the butterfly in λ and η determines the 5-jet, i.e., $j^5 f(0) \sim_{\mathcal{A}} (x, xy + y^5)$, and there is an additional open condition on 7-jets which detects the $\mathcal{A}$-type exactly (indeed the butterfly is 7-$\mathcal{A}$-determined). The other cases are also similar. A complete set of criteria for $\mathcal{A}$-types with higher codimension becomes more involved – that is achieved in [9] for $\mathcal{A}_e$-codimension ≤ 4. For our purpose, Table 3 is sufficient: by checking the conditions, we will find systematically the defining equation of each local singularity stratum in the bifurcation diagram of corank two germs.

2.2. **Sharksfin.** We prove Theorem 1.1. The normal form of the sharksfin presented in Introduction is inconvenient for computing the swallowtail locus in the bifurcation diagram (As mentioned before, the computation was not successful in [6]). Instead, we take an alternative $\mathcal{A}$-equivalent form $(xy, x^2 + y^2 + x^3)$ and the $\mathcal{A}$-miniversal unfolding

$$F(x, y, s, t) = (xy, x^2 + y^2 + x^3 + sx + ty). \tag{3}$$

This normal form behaves nicely – the computation is drastically simplified. Below we describe the bifurcation diagram in the st-space for this versal unfolding by using the criteria in Table 3. Set

$$\lambda := \det(dF_{s,t}) = \begin{vmatrix} y & x \\ s + 2x + 3x^2 & t + 2y \end{vmatrix}$$

and $\eta := x\frac{\partial}{\partial x} - y\frac{\partial}{\partial y}$, unless $x = y = 0$ (set $\eta = t\frac{\partial}{\partial x} - s\frac{\partial}{\partial y}$, otherwise).

The swallowtail locus is given by three algebraic equations in variables x, y, s, t

$$\lambda = \eta\lambda = \eta\eta\lambda = 0$$

(open conditions automatically hold near the origin). We are seeking for an equation in s, t by eliminating x, y from these equations; Our trick is *to eliminate s, t first*, that is actually the right way. Let $(x, y, s, t) \neq 0$. By $\eta\lambda = \eta\eta\lambda = 0$, it is easy to have

$$s = -\tfrac{2}{x}(3x^2 + 9x^3 - y^2), \;\; t = \tfrac{1}{y}(2x^2 + 9x^3 - y^2)$$

(if $x = 0$ or $y = 0$, these equations implies $x = y = s = t = 0$). Substitute them into the remaining equation $\lambda = 0$, then we have $y^2 = x^2 + 4x^3$, hence $y = \pm x\sqrt{1 + 4x}$ around the origin. Then the parameter values s, t are determined:

$$s = -4x - 10x^2, \;\; t = \pm x(4 + 15x)(1 + 4x)^{-1/2}.$$

Eliminating x we obtain the desired equation: the analytic branches at the origin are given by

$$\pm t = s + \tfrac{3}{16}s^2 + \tfrac{9}{64}s^3 + \tfrac{155}{1024}s^4 + O(5).$$

Next, let us see the beaks/lips types. The condition $d\lambda = 0$ (i.e., $\frac{\partial}{\partial x}\lambda = \frac{\partial}{\partial y}\lambda = 0$) implies that

$$s = -4x - 9x^2, \;\; t = -4y.$$

Substitute them into $\lambda = 0$, then it yields that $y^2 = x^2 + 3y^3$, hence $y = \pm x\sqrt{1 + 3x}$ around the origin. Since $\mathrm{H}_\lambda(0) = -4 < 0$ and $\eta\eta\lambda(0) \neq 0$, it is actually of type beaks, not of type lips (see the criteria in Table 3): Hence there is no lips locus, and the beaks locus is expressed by

$$\pm t = s + \tfrac{3}{16}s^2 + \tfrac{9}{64}s^3 + \tfrac{621}{4096}s^4 + O(5).$$

Note that branches of the beaks and the swallowtail have 4-point contact, i.e., the difference is given by $t = \pm\frac{1}{4096}s^4 + O(5)$.

There do not appear other $\mathcal{A}$-types of mono and multi-singularities, as mentioned in Introduction (cf. [6]). Hence the bifurcation diagram in the st-space of the unfolding (3) consists of four smooth curves passing through the origin, which correspond to types beaks and swallowtail just as described, and is transformed to the bifurcation diagram in the ab-space of the normal form (1) by some diffeomorphism $(s, t) \mapsto (a, b)$. Since the beaks is given by $ab = 0$ (directly checked by the form (1)), the above argument implies that the swallowtail locus is given by $b = \delta a^4 + \cdots$ and $a = \delta b^4 + \cdots$ for some positive constant δ. In fact, by writing down the linear part of the change of parameters, we see $\delta = \frac{1}{16}$. This completes the proof.

Remark 2.2. One can prove Theorem 1.1 using the normal form (1) instead of (3) in the same way as above; it however requires a long computer-aided calculation for computing the swallowtail locus [22].

2.3. **Odd-shaped sharksfin.** Let us take the miniversal unfolding (2) of the odd-shaped sharksfin

$$F(x, y, a, b, c) = F_{a,b,c}(x, y) = (x^2 + y^5 + cy^3 + ay, y^2 + x^3 + bx),$$

and put

$$\lambda := \det(dF_{a,b,c}) = \begin{vmatrix} 2x & 5y^4 + 3cy^2 + a \\ 3x^2 + b & 2y \end{vmatrix}.$$

The differential $dF_{a,b,c} = O$ if and only if $a = b = x = y = 0$, thus the c-axis in the abc-space corresponds to the locus of sharkskin. It is also easy to see that $\lambda = 0$ and $d\lambda = 0$ if and only if $ab = 0$ and $x = y = 0$. Then, $\det \mathrm{H}_\lambda(0) = 36abc - 16 < 0$, thus the lips and the goose do not appear, and

- If $a = 0$ and $b \neq 0$, set $\eta := -2y\frac{\partial}{\partial x} + (3x^2 + b)\frac{\partial}{\partial y}$, then $\eta^2\lambda(0) = -6b^3c$, and $\eta^3\lambda(0) = -24b^2 \neq 0$; hence the gulls occurs if $c = 0$, and the beaks does, otherwise.
- If $a \neq 0$ and $b = 0$, set $\eta := -(5y^4 + 3cy^2 + a)y\frac{\partial}{\partial x} + 2x\frac{\partial}{\partial y}$, then $\eta^2\lambda(0) = -6a^3 \neq 0$; thus the beaks appears but the gulls does not.

Next let us see the swallowtail. The germ $(F, a, b, c) : \mathbb{R}^5, 0 \to \mathbb{R}^5, 0$ is the one-dimensional suspension of a stable germ of type $I_{2,2}$, hence $\Sigma^{1,1,1}(F)$ is not adjacent to the origin and the $\Sigma^{1,1}(F)$ is the one-dimensional suspension of a nodal curve in $\mathbb{R}^5$ (Lander [10, Lem 3.6], [12]); projecting to the abc-space, the butterfly does not appear in $\mathcal{B}_F$, and the swallowtail stratum is formed by two smooth surfaces with transverse intersection along the c-axis. It follows from Theorem 1.1 that these two surfaces must be tangent to the planes $a = 0$ and $b = 0$ (i.e., the beaks locus) with 4-point contact along the c-axis off the origin (it is not needed to know the defining equations of the surfaces explicitly).

As for multi-singularity strata, it is enough to consider the tacnode folds by the same reason as the case of sharksfin. The locus is defined by conditions in variables x, y, X, Y, a, b, c so that two points (x, y) and (X, Y) are distinct but have the same image of $F_{a,b,c}$, and that the matrix

$$\begin{bmatrix} 2x & 5y^4 + 3cy^2 + a & 2X & 5Y^4 + 3cY^2 + a \\ 3x^2 + b & 2y & 3X^2 + b & 2Y \end{bmatrix}$$

has rank one (six minors vanish), e.g., the minor of first and third columns gives an equation $(X - x)(b - 3xX) = 0$. We easily find the solution

$$4a = c^2 \ (c < 0), \quad X = x = 0, \quad Y = -y \ = \pm\sqrt{-c/2}.$$

In fact, if $X = x$, the solution is immediately obtained; If $b = 3xX$, the other minors show $xy = XY = xY = Xy = 0$, that leads to $X = x = 0$.

As a summary, in the abc-space, the beaks locus consists of two planes defined by $ab = 0$; the gulls is the b-axis; the sharksfin is the c-axis; the swallowtail locus consists of two smooth surfaces being tangent to the beaks planes along the c-axis (4-point contact), one of which is also tangent to the bc-plane along the b-axis (3-point contact); and the tacnode fold is the suspension of one half of the parabola. Using the bifurcation diagram of sharksfin described in the previous section (Fig.3) and the bifurcation diagram of gulls (cf. [6, §5]), we obtain Fig.7.

2.4. **More degenerate sharksfin.** Consider $I^{2,2}_{2,2}$ of $\mathcal{A}_e$-codimension 4. Its $\mathcal{A}$-miniversal unfolding is given by

$$F(x, y, a, b, c, d) = (x^2 + y^5 + cy^3 + ay, y^2 + x^5 + dx^3 + bx). \tag{4}$$

In entirely the same way as in §2.3, we see that in the $abcd$-space, the cd-plane ($a = b = 0$) corresponds to $I_{2,2}$ - the c and d-axes are of odd-shaped sharksfin, and the complement corresponds to the sharksfin; the beaks is defined by $ab = 0$; the swallowtail is formed by two smooth irreducible hypersurfaces having transverse intersection along the cd-plane; the gulls is the union of two planes of $a = c = 0$ and $b = d = 0$; the tacnode fold is the union of two copies of half of the parabola,

$4a = c^2$ ($c < 0$) and $4b = d^2$ ($d < 0$). The butterfly, the goose and more degenerate local singularities (and other multi-singularity types) do not appear.

Let us make a picture of the intersection of the bifurcation diagram $\mathcal{B}_F$ with some typical hypersurface in the *abcd*-space $\mathbb{R}^4$; we consider $V_0 = \{(a, b, c(t), d(t)) \in \mathbb{R}^4\}$ parametrized by a, b and t so that $(c(t), d(t)) : \mathbb{R}, 0 \to \mathbb{R}^2, 0$ is an immersed curve-germ in the *cd*-plane with positive slope (i.e., $c(t)d(t) > 0$ for t small enough), e.g., the hyperplane in $\mathbb{R}^4$ given by $c = d = t$, and also consider V_1 for negative slope, e.g., the hyperplane $c = -d = t$. These hypersurfaces V_i are transverse to any strata of $\mathcal{B}_F$ off the origin. We identify each V_i with the *abt*-space and depict the sections $\mathcal{B}_i := \mathcal{B}_F \cap V_i$ ($i = 0, 1$) in the *abt*-space, see Fig.12: the locus of sharksfin is the t-axis; the locus of gulls is the union of a and b-axes; the beaks is the union of two planes $ab = 0$; the swallowtail consists of two smooth surfaces tangent to the two planes of beaks along the a and b-axes; finally the tacnode is defined by $4a = c(t)^2$, $c(t) < 0$ and $4b = d(t)^2$, $d(t) < 0$. Notice that the placement of the tacnode strata depends on the sign of $c(t)$ and $d(t)$, thus their pictures for $i = 0, 1$ differ from each other. Also the placement of swallowtail depends on $i = 0, 1$. These pictures will be used in the later section.

The bifurcation diagram of $II^2_{2,2}$ is reduced from the one of the deltoid $II^1_{2,2}$. In the source 6-space of its $\mathcal{A}$-miniversal unfolding, the *ab*-plane is normal to $\Sigma^{2,0}$ and there is no adjacency of $\Sigma^{1,1,1}$ ([10]); the bifurcation diagram in *abcd*-space consists only of the *cd*-plane corresponding to the deltoid type. The case of $II^n_{2,2}$ ($n > 2$) is similar.

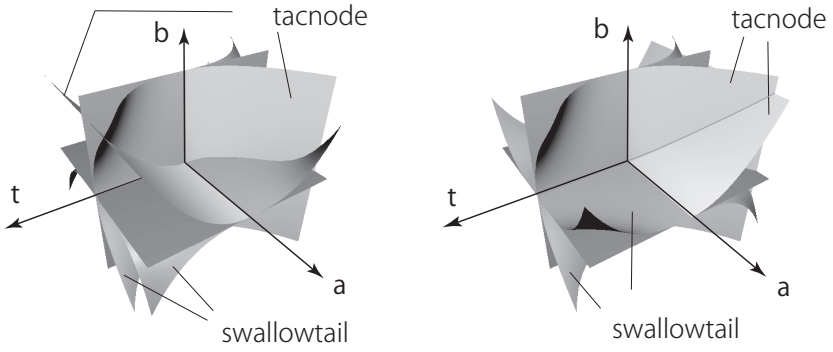

FIGURE 12. Bifurcation diagrams restricted to the hypersurfaces V_i: $\mathcal{B}_0 \subset V_0$ (right) and $\mathcal{B}_1 \subset V_1$ (left) where each V_i is identified with the *abt*-space.

3. Central Projection of Crosscap

3.1. **Proof of Theorem 1.3.** First we consider the action of the subgroup with linear target changes $\mathrm{Diff}(\mathbb{R}^2, 0) \times GL_3 \subset \mathcal{A}_{2,3}$ on the ℓ-jet space $J^\ell(2, 3)$.

Let $f : \mathbb{R}^2, 0 \to \mathbb{R}^3, 0$ be a germ of crosscap. Since f is of corank 1 and the 1-jet extension is transverse to Σ^1, by some linear change of the source and the target we may assume

$$f(x, y) = (x, xy + O(3), y^2 + \alpha x^2 + O(3))$$

where $\alpha = 1$, $\alpha = -1$ or $\alpha = 0$; We say that the crosscap f is *elliptic*, *hyperbolic* or *parabolic*, respectively ([21, 20]). By a further coordinate change of the source and a linear change of the target, we may write

$$f(x,y) = (x, xy + g(y), y^2 + \alpha x^2 + \phi(x,y)) + O(\ell+1) \tag{5}$$

for some $g(y) = \sum_{i\geq 4} d_i y^i$ and $\phi(x,y) = \sum_{i+j\geq 3} c_{ij} x^i y^j$ (cf. [21]). We call it the *affine normal form* of crosscap.

Let $\iota : M \to \mathbb{R}^3$ be a smooth map having a crosscap at $x_0 \in M$ with $\iota(x_0) \neq 0$, and $U \subset \mathbb{R}^3 - M$ a small neighborhood of the origin. We are concerned with the family of central projections

$$\varphi : M \times U \to \mathbb{R}P^2, \;\; \varphi(x,p) = \varphi_p(x) := \pi_p \circ \iota(x),$$

where $p = (u,v,w) \in U$ is a viewpoint. Of our particular interest is its corank 2 singularity.

Taking a local coordinates of M centered at x_0 and an affine transform of $\mathbb{R}^3$, we may assume that $\iota(x_0) = (1,0,0)$ and ι is locally written by

$$\iota(x,y) = \left(1 + x, xy + g(y), y^2 + \alpha x^2 + \phi(x,y)\right),$$

using the affine normal form (5); we have

$$\varphi(x,y,u,v,w) = \left(\frac{xy + g(y) - v}{1 + x - u}, \frac{y^2 + \alpha x^2 + \phi(x,y) - w}{1 + x - u} \right).$$

Clearly, $\varphi_p(x,y)$ has a corank 2 singularity if and only if the viewpoint p lies on the u-axis, so we now assume that $v = w = 0$. Then, coefficients of the Taylor expansion of $\varphi_p(x,y)$ at the origin are expressed in terms of u, d_j, c_{ij}.

Let $\alpha = 0$, i.e., take a parabolic crosscap; this yields a closed condition on the space of jets of all crosscap-germs ι, so it does not generically occur.

On the other hand, elliptic and hyperbolic crosscaps are generic. Let $\alpha = +1$. Substitute $x = \bar{x} + \bar{y}$ and $y = \bar{x} - \bar{y}$, then by some coordinate change of the source and a linear change of the target, we have

$$\varphi_p(x,y) = \left(x^2 + \frac{A}{4(1-u)^2} y^3 + O(4), y^2 + \frac{B}{4(1-u)^2} x^3 + O(4) \right)$$

where

$$A = c_{03} - c_{12} + c_{21} - c_{30}, \;\; B = c_{03} + c_{12} + c_{21} + c_{30}.$$

Both A and B are not equal to zero if and only if $\varphi_p \sim_{\mathcal{A}} (x^2 + y^3, y^2 + x^3)$. $A = 0$ or $B = 0$ gives a relation among coefficients c_{ij}'s, that causes a closed condition on the space of jets of crosscap-germs ι, thus such a case does not generically occur. In case that $\alpha = -1$, we can easily see that $\varphi_p \sim_{\mathcal{A}} (xy, x^2 - y^2 + y^3)$ as long as $c_{03} \neq 0$.

This completes the proof of Theorem 1.3.

3.2. **Affine geometry of crosscap.** We deal with the affine geometry of crosscap given by the normal form (5) from singularity theory approach; we are concerned with two characteristic curves on a singular surface $\iota(M) \subset \mathbb{R}^3$ with a crosscap – the parabolic curve and the flecnodal curve. We prove Theorem 1.4, and show that these curves actually lie on the surface like as Fig.10.

As mentioned before, the parabolic curve and the flecnodal curve are characterized as the loci at which the parallel projection along asymptotic lines admit beaks and swallowtail singularity types, respectively. These curves do not approach to any

hyperbolic crosscap, since the singularity of the projection along the tangent line at the crosscap is of type $II_{2,2}$ which has no adjacencies of beaks and swallowtail types (cf. §2.4). Thus we consider elliptic crosscaps from now on. Let $\varphi : M \times U \to \mathbb{R}^2$ be the parallel projection:

$$\varphi(x, y, v, w) = \big(xy - vx + g(y), x^2 + y^2 - wx + \phi(x, y)\big)$$

where $g(y) = d_4y^4 + \cdots$ and $\phi(x, y) = c_{30}x^3 + c_{21}x^2y + c_{12}xy^2 + c_{03}y^3 + \cdots$.

3.2.1. **Parabolic curve.** Put $\lambda = \det \varphi_{v,w}$, then the beaks singularity is characterized by three equations, $\lambda = \frac{\partial}{\partial x}\lambda = \frac{\partial}{\partial y}\lambda = 0$. They provide an equation in x, y by eliminating v, w, which is the defining equation of the parabolic curve in the source xy-space:

$$\begin{aligned}
&x^2 - y^2 + (3c_{03} + 2c_{21})x^2y + (c_{12} + 3c_{30})x^3 - 3c_{03}y^3\\
&+(-\tfrac{1}{4}c_{21}^2 + c_{22} + 3c_{12}c_{30} + 6c_{40})x^4 + (3c_{13} + c_{12}c_{21} + 9c_{03}c_{30} + 5c_{31})x^3y\\
&+(6c_{04} + \tfrac{9}{2}c_{03}c_{21} + 3c_{22})x^2y^2 - 4d_4xy^3 - (\tfrac{9}{4}c_{03}^2 + 4c_{04})y^4 + h.o.t = 0.
\end{aligned}$$

An alternative way is to compute the second fundamental form of the surface with respect to a fixed Euclidean metric; the equation $LN - M^2 = 0$ (the second fundamental form) gives the same answer. This curve has a nodal point at the origin and two analytic branches are expressed by

$$\begin{aligned}
y &= y_{p,\pm}(x)\\
&= \pm x + \tfrac{1}{2}(\pm c_{12} + 2c_{21} \pm 3c_{30})x^2\\
&\quad +\tfrac{1}{8}\begin{pmatrix} \mp 9c_{03}^2 - 12c_{03}c_{12} \mp c_{12}^2 \mp 6c_{03}c_{21}\\ +4c_{12}c_{21} \pm 3c_{21}^2 \pm 6c_{12}c_{30} \mp 9c_{30}^2\\ \pm 8c_{04} + 12c_{13} \pm 16c_{22} + 20c_{31} \pm 24c_{40} - 16d_4 \end{pmatrix} x^3 + O(4).
\end{aligned}$$

Indeed, the expansion up to order 3 is determined by the 4-jet of the above equation, and this is verified by substitution.

3.2.2. **Flecnodal curve.** Put $\eta = x\frac{\partial}{\partial x} - (y - v)\frac{\partial}{\partial y}$. The swallowtail singularity is characterized by three equations $\lambda = \eta\lambda = \eta\eta\lambda = 0$. It is however hard to obtain an equation in x, y from these equations by eliminating v, w. On the other hand, by a similar argument in the proof of Theorem 1.1 (also [10, 12]), we see that the solution in $xyvw$-space defines two smooth curve-germs at the origin. Then, from a bit long computation for power series solutions, we obtain the following expression of two branches in xy-plane:

$$\begin{aligned}
y &= y_{i,\pm}(x)\\
&= \pm x + \tfrac{1}{2}(\pm c_{12} + 2c_{21} \pm 3c_{30})x^2\\
&\quad +\tfrac{1}{4}\begin{pmatrix} \mp 4c_{03}^2 - 5c_{03}c_{12} \mp 2c_{03}c_{21} + 3c_{12}c_{21}\\ \pm 2c_{21}^2 + c_{03}c_{30} \pm 4c_{12}c_{30} + c_{21}c_{30} \mp 4c_{30}^2\\ \pm 4c_{04} + 6c_{13} \pm 8c_{22} + 10c_{31} \pm 12c_{40} - 8d_4 \end{pmatrix} x^3 + O(4).
\end{aligned}$$

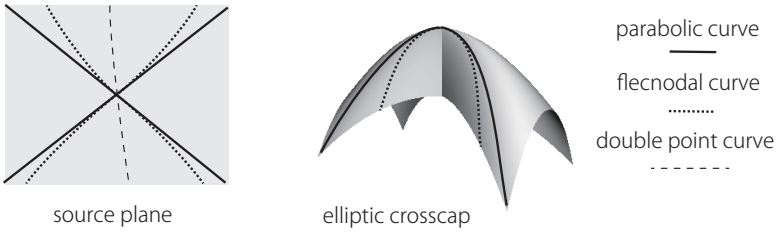

FIGURE 13. Two characteristic curves on a generic elliptic crosscap

Also v, w are expressed in x as

$$\begin{aligned} v &= \mp 2x + \tfrac{1}{2}(-2c_{03} \mp c_{12} + 4c_{21} \mp 7c_{30})x^2 \\ &\quad + \begin{pmatrix} -2c_{03}c_{12} \pm 3c_{03}c_{21} + c_{12}c_{21} \mp c_{21}^2 \\ -3c_{03}c_{30} \mp c_{12}c_{30} \pm 3c_{30}^2 \\ +2c_{13} \mp 4c_{22} + 6c_{31} \mp 8c_{40} + \frac{4}{3}d_4 \end{pmatrix} x^3 + O(4) \\ w &= 4x + (\mp c_{03} + 4c_{12} \mp 7c_{21} + 10c_{30})x^2 \\ &\quad + \begin{pmatrix} -3c_{03}^2 \pm 4c_{03}c_{12} + 2c_{12}^2 \mp 10c_{12}c_{21} + 7c_{21}^2 \\ \mp 6c_{03}c_{30} + 14c_{12}c_{30} \mp 12c_{21}c_{30} \\ +4c_{04} \mp 8c_{13} + 12c_{22} + \mp 16c_{31} \mp 20c_{40} \pm \frac{16}{3}d_4 \end{pmatrix} x^3 + O(4), \end{aligned}$$

where the double sign corresponds to the double sign in y above. A simple substitution verifies that the above parametrizations of y, v, w in x satisfy the defining equations $\lambda = \eta\lambda = \eta\eta\lambda = 0$ (up to 3-jets). Tracing the curve $(v(x), w(x))$ on the parameter space and the curve $\iota(x, y_{i,\pm}(x))$ on the singular surface, we see that the asymptotic lines (singular view lines) in 3-space are placed as in Fig.10 in Introduction.

3.2.3. **Proof of Theorem 1.4.** Compare the flecnodal curve $y = y_{i,\pm}(x)$ and the parabolic curve $y = y_{p,\pm}(x)$ in xy-plane; they coincide up to degree 2, and the difference of cubic terms are surprisingly simplified:

$$y_{p,-} - y_{i,-} = \tfrac{1}{8}A^2x^3 + O(4), \quad y_{p,+} - y_{i,+} = -\tfrac{1}{8}B^2x^3 + O(4)$$

where $A = c_{03} - c_{12} + c_{21} - c_{30}$ and $B = c_{03} + c_{12} + c_{21} + c_{30}$. Thus from the proof of Theorem 1.3 given in the previous subsection, we see that the following properties are equivalent: (1) in the source plane parametrizing the crosscap, these smooth branches of the parabolic curve and the flecnodal curve have 3-point contact; (2) both A and B are not zero; (3) the elliptic crosscap is generic, i.e., the projection is of type sharksfin.

Moreover, in case that $A = 0$ and/or $B = 0$, the contact order becomes to be an odd number greater than three, since the flecnodal curve must be placed in the hyperbolic domain $LN - M^2 = x^2 - y^2 + \cdots < 0$ (see Fig.13).

As a remark, the parabolic curve and the flecnodal curve on the singular surface $\iota(M) \subset \mathbb{R}^3$ have 4-point contact at the crosscap point of generic elliptic type:

$$\begin{gathered} \iota(x, y_{i,\pm}(x)) - \iota(x, y_{p,\pm}(x)) = \\ (0, -\tfrac{1}{8}A^2x^4, \tfrac{1}{4}A^2x^4) + O(5), \quad (0, \tfrac{1}{8}B^2x^4, \tfrac{1}{4}B^2x^4) + O(5). \end{gathered}$$

This completes the proof of Theorem 1.4.

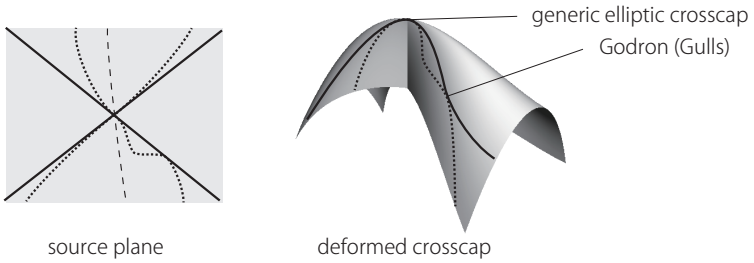

FIGURE 14. Non-generic elliptic crosscap is deformed to a generic one with producing a tangential point (gulls) of the parabolic curve and the flecnodal curve.

3.2.4. **Non-generic elliptic crosscap.** The order of tangency between (components of) the parabolic curve and the flecnodal curve defines a new affine differential invariant of crosscap: we conjecture that for elliptic crosscaps, the order of tangencies of these component curves (in the source M) are $2\ell+1$ and $2m+1$, respectively, if and only if the projection along the image tangent line is $\mathcal{A}$-equivalent to the type $I^{\ell,m}_{2,2}$. Of course the case of $\ell = m = 1$ is proved in Theorem 1.4. It seems that our conjecture also relates to a result of [15, Thm. 2.3] on the torsion of parametrized parabolic curves near crosscap as space curves.

If $A = 0$ or $B = 0$ (i.e, ℓ or $m > 1$), then the projection surely has a worse singularity than the sharksfin $I^{1,1}_{2,2}$. As shown in Theorem 1.3, such a singularity does not appear generically, but for instance, the odd-shaped sharksfin $I^{2,1}_{2,2}$ can appear in projection when one generically deforms the singular surface with one parameter, say $M \times \mathbb{R} \to \mathbb{R}^3$, $(x,t) \mapsto \iota_t(x)$. Assume that the map ι_0 has such a non-generic elliptic crosscap point at $x_0 \in M$, and that ι_t for $t \neq 0$ has only generic elliptic crosscap. Then, in the source of ι_0, a branch of the flecnodal curve has 5-point contact with the parabolic curve at the point x_0. As the parameter t varies from 0, the non-generic crosscap breaks into a generic elliptic crosscap (at which the branches of parabolic and flecnodal curves meet each other with 3-point contact) and a tangential point of these two branches (2-point contact), see Fig.14. At the latter point, the projection along the asymptotic line has the singularity of gulls. This bifurcation of non-generic crosscap is nothing but the deformation of a generic section for the odd-shaped sharksfin which has been depicted in Fig.8 in Introduction.

4. Sections of bifurcation diagram of corank 2

4.1. **Bifurcation of planar caustics.** As mentioned in Introduction, there are two types of D^+_4-perestroika of planar caustics which are embedded in the miniversal unfolding of the sharksfin (Fig.11). We seek for analogous 2-dimensional families of caustics.

First, we consider a stable Lagrange map-germ $\Phi : \mathbb{R}^4, 0 \to \mathbb{R}^4, 0$ [2]: let $U(x, y, q_1, q_2)$ be a family of functions in x, y of type A_k $(1 \leq k \leq 5)$, D_4 or D_5 without linear terms, then it generates Φ by

$$\Phi : (x, y, q_1, q_2) \mapsto (\mu_1, \mu_2, q_1, q_2), \quad \mu_1 = \frac{\partial U}{\partial x}, \ \mu_2 = \frac{\partial U}{\partial y}$$

(the generating family is given by $U-\mu_1 x-\mu_2 y$). The critical value set D_Φ is called a *big caustics* in 4-space. As a natural generalization of perestroikas of caustics [2, 24], a 2-*parameter bifurcation of planar caustics* is defined by the diagram

$$\mathbb{R}^4,0 \xrightarrow{\Phi} \mathbb{R}^4,0 \xrightarrow{\rho} \mathbb{R}^2,0$$

of the above Φ and a submersion-germ ρ so that the composed map-germ $\rho\circ\Phi : \mathbb{R}^4,0 \to \mathbb{R}^2,0$ is also a submersion. The last condition means that each section $D_\Phi \cap \rho^{-1}(t)$ of the big-caustics via a level set is diffeomorphic to a planar caustics of some Lagrange map. Two diagrams (Φ_i,ρ_i) $(i=1,2)$ are *equivalent* if there are diffeomorphism germs σ,τ,h of the source, the target and the parameter space, respectively, so that $\Phi_2\circ\sigma=\tau\circ\Phi_1$ and $\rho_2\circ\tau=h\circ\rho_1$. We also say that they are *topologically equivalent* if such σ,τ,h are homeomorphisms.

The bifurcation diagram of (Φ,ρ) is defined to be the set of parameters $t\in\mathbb{R}^2$ so that $D_\Phi\cap\rho^{-1}(t)$ is an unstable caustics.

We would not attempt to classify the diagrams here (it is outside of our purpose in this paper); instead we are interested in finding some non-trivial examples of bifurcations of D_4-type caustics as an application of the study in the previous sections on (degenerate) odd-shaped sharksfin.

4.2. **D_4^+-type bifurcations.** Let us consider the D_4^+-type:

$$U(x,y,q_1) := \tfrac{1}{3}y^3+\tfrac{1}{2}x^2y+\tfrac{1}{2}q_1y^2.$$

Then $\mu_1=\frac{\partial U}{\partial x}=xy$ and $\mu_2=\frac{\partial U}{\partial y}=x^2+y^2+q_1y$.

4.2.1. **D_4^+-perestroika** [2, 24]**.** Consider the diagram

$$\mathbb{R}^3,0\to\mathbb{R}^3,0\to\mathbb{R},0,\quad (x,y,q_1)\mapsto(\mu_1,\mu_2,q_1)\mapsto t:=q_1-\mu_1.$$

Substituting $q_1=t+\mu_1$ into the function μ_2, the first map-germ $\mathbb{R}^3,0\to\mathbb{R}^3,0$ is $\mathcal{A}$-equivalent to

$$(x,y,t)\to(xy,x^2+y^2+ty+xy^2,t)$$

(it does not mean parametric equivalence). The obtained map has the form of a one-parameter unfolding of the germ $(xy,x^2+y^2+xy^2)$, which is of type sharksfin, therefore this is (parametrically) $\mathcal{A}$-equivalent to an induced family from the $\mathcal{A}$-miniversal unfolding F of the form (1) in Introduction via some smooth curve-germ $t\mapsto(a(t),b(t))$ in the ab-plane. It is not difficult to see that the curve-germ is tangent to the diagonal line $a=b$, hence from Fig.3 (between no.1 and no.7), our diagram actually corresponds to the D_4^{+1}-perestroika of planar caustics in Fig.11. Take $t:=q_1-\mu_2$ instead, then $\mu_2=\frac{1}{1-y}(x^2+y^2+ty)$, and by some coordinate change, we may write the first map by

$$(x,y,t)\to(xy,x^2+y^2+ty+y^3,t).$$

This is also an unfolding of type sharksfin; indeed this is a one-parameter family induced from (1) via a curve tangent to $a=-b$, which corresponds to the D_4^{+2}-perestroika (between no.4 and no.11 in Fig.3). More generally, we may take $t:=q_1-\mu_1-r\mu_2$ or $t:=q_1-\mu_2-r\mu_1$, then we have a family induced form F via a curve with another slope, which is *topologically equivalent* to the induced family via $a=\pm b$ as above. In fact, r corresponds to a moduli parameter arising in the normal form of generating family for the D_4^+-perestroika given by Zakalyukin [24] (Theorem in §3 of that paper with $n=2$).

4.2.2. **Two parameter D_4^+-type bifurcations.** We extend the above observation to the case of 2-parameter families. Adding a trivial parameter q_2, we have

$$\Phi : \mathbb{R}^4, 0 \to \mathbb{R}^4, 0, \ \ \Phi(x, y, q_1, q_2) = (xy, x^2 + y^2 + q_1 y, q_1, q_2).$$

Define a submersion $\rho = (t_1, t_2) : \mathbb{R}^4, 0 \to \mathbb{R}^2, 0$ by sending (μ_1, μ_2, q_1, q_2) to

$$t_1 = q_1 - q_2\mu_1 - \mu_1^2, \quad t_2 = q_2.$$

Let us substitute $q_1 = t_1 + t_2\mu_1 + \mu_1^2$, $q_2 = t_2$ in Φ, then the diagram (Φ, ρ) is equivalent to the diagram (G, pr) where

$$G : \mathbb{R}^4, 0 \to \mathbb{R}^4, 0, \ \ (x, y, t_1, t_2) \to (\mu_1, \mu_2, t_1, t_2)$$

is given by

$$\mu_1 = xy, \ \ \mu_2 = x^2 + y^2 + t_1 y + t_2 xy^2 + x^2 y^3,$$

and $pr(x, y, t_1, t_2) = (t_1, t_2)$. We now regard G as a 2-parameter unfolding of the plane-to-plane germ $g = G(x, y, 0, 0)$. Note that

$$g = (xy, x^2 + y^2 + x^2 y^3) \sim_{\mathcal{A}} (x^2 + y^5, y^2 + x^5) =: f,$$

which is of type $I^{2,2}_{2,2}$, thus G is obtained from the $\mathcal{A}$-miniversal unfolding F of f given by the normal form (4) in §2.4. That is, G is (parametrically) $\mathcal{A}$-equivalent to the induced family from F via some map-germs $(t_1, t_2) \mapsto (a, b, c, d)$.

By finding explicitly (jets of) coordinate changes to transform g to f, we see that infinitesimal deformations $\frac{\partial}{\partial t_1}G|_{t_1=0} (= y\frac{\partial}{\partial v})$ and $4\frac{\partial}{\partial t_2}G|_{t_2=0} (= 4xy^2\frac{\partial}{\partial v})$ in $\theta(g)/T\mathcal{A}_e.g$ correspond to $y\frac{\partial}{\partial u} + x\frac{\partial}{\partial v}$ and $-y^3\frac{\partial}{\partial u} + x^3\frac{\partial}{\partial v}$ in $\theta(f)/T\mathcal{A}_e.f$, respectively, where (u, v) denote coordinates of the target $\mathbb{R}^2$. This implies that the t_1t_2-parameter space of G can be embedded into the parameter 4-space of the versal unfolding F such as $(a, b, c, d) = (t_1, t_1, -\frac{1}{4}t_2, \frac{1}{4}t_2) + h.o.t.$. In particular, if $t_1 = 0$, the t_2-curve lies on the cd-plane: $(c(t), d(t)) = \frac{1}{4}(-t, t) + O(2)$ with $t = t_2$. Now we take the hypersurface $V_1 \subset \mathbb{R}^4$ defined in §2.4 using this t_2-curve (the slope is negative) and indentify V_1 with the abt-space. The bifurcation diagram $\mathcal{B}_F$ induces the restriction $\mathcal{B}_1$ in the abt-space $(= V_1)$, see the left in Fig.12. Then G defines a smooth surface in the abt-space, which is tangent to the plane $a = b$, contains the t-axis, and is transverse to any strata of $\mathcal{B}_1$ off the t-axis, see the right in Fig.15. Thus the bifurcation diagram of G in the t_1t_2-space is obtained as the intersection of $\mathcal{B}_1$ with the surface depicted by the left in Fig.15.

The diagram (Φ, ρ) above should be *generic* in an appropriate sense. Here is a rough sketch: When perturbing ρ slightly (with fixing Φ as above), G is slightly perturbed. The component function μ_1 of G does not change and μ_2 is added by terms of $xy^2, (x^2 + y^2)y$ and more higher, and these new terms correspond to the direction $xy^2\frac{\partial}{\partial v}$ or zero in the normal space to $T\mathcal{A}_e g$. Thus the perturbation of ρ simply causes a small perturbation of the 2-dimensional section in the abt-space V_1 preserving the t-axis; the resulting section must be topologically equivalent to the original one.

In the same way, we may find another 2-dimensional sections of the bifurcation diagram of type $I^{2,2}_{2,2}$. Indeed there are at least four choices so that the t_1-curve is tangent to $a = \pm b$ and the t_2-curve is tangent to $d = \pm c$. The above case corresponds to $a = b$ and $c = -d$. The other three cases are also realized by choosing ρ appropriately. For instance, take ρ such as $t_1 = q_1 - q_2\mu_2 - \mu_1^2$ and

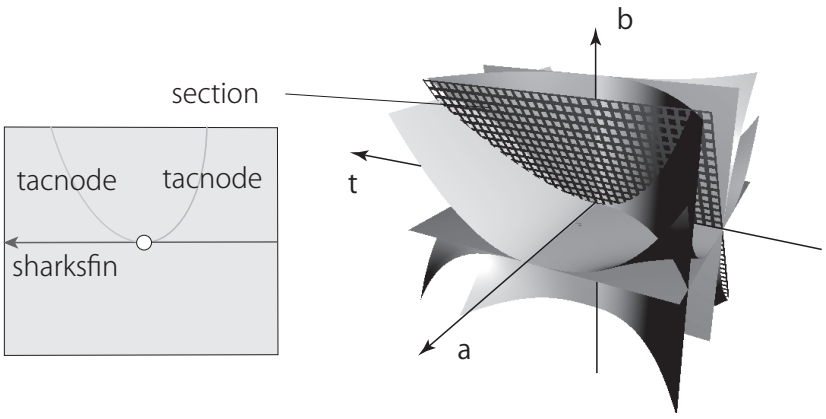

FIGURE 15. A 2-dimensional bifurcation of planar caustics corresponding to a section of $\mathcal{B}_1 = \mathcal{B}_F \cap V_1$.

$t_2 = q_2$; by some coordinate changes, G may be of the form

$$\mu_1 = xy, \quad \mu_2 = x^2 + y^2 + t_1 y + t_2 y^3 + x^2 y^3.$$

Then the unfolding G embeds the t_1t_2-space into a hypersurface V_0 defined in §2.4, that corresponds to the case that $a = b$ and $c = d$. The remaining two cases are also obtained by some sections of $\mathcal{B}_i$ $(i = 0, 1)$, that correspond to the cases that $a = -b$ and $c = \pm d$.

The bifurcation diagrams are drawn in Fig.16, which are immediately obtained by taking the intersection of two planes $a = \pm b$ and $\mathcal{B}_i = \mathcal{B}_F \cap V_i$ $(i = 0, 1)$ in Fig.12. These families are new examples as a fairly natural extension of the D_4^+-perestroikas of planar caustics (Fig.11).

Finally we conjecture that for any generic submersion ρ with respect to Φ being fixed as above, the diagram (Φ, ρ) is topologically equivalent to one of the above four types, and also that for each of four types, the diagram (Φ, ρ') with a sufficiently small perturbation ρ' of the submersion given above is still topologically equivalent to the original one. That is to say, generic 2-dimensional bifurcations of planar caustics of type D_4^+ are conjecturally only of these four types. A right proof should be given by classifying submersion-germs ρ via diffeomphisms preserving the big caustics D_Φ in extending the approach of [24].

REFERENCES

[1] V. I. Arnold, Indices of singular points of 1-forms on manifolds with boundary, convolution of invariants of groups, generated by reflections, and singular projection of smooth hyper surfaces, Russian Math. Surveys 34 no. 2 (1979), 1–42.
[2] V. I. Arnold, Singularities of caustics and wavefronts, Kluwer Acad. Publ. (1991).
[3] V. I. Arnold, Catastrophe Theory, 3rd edition, Springer (2004).
[4] J. W. Bruce, Projections and reflections of generic surfaces in $\mathbb{R}^3$, Math. Scand. 54 (1984), 262–278.
[5] T. Fukui and M. Hasegawa, Singularities of parallel surfaces, Tohoku Math. J. (2), 64, (2012), 387-408.
[6] C. G. Gibson and C. A. Hobbs, Singularity and Bifurcation for General Two Dimensional Planar Motions, New Zealand J. Math. , 25 (1996) 141–163.

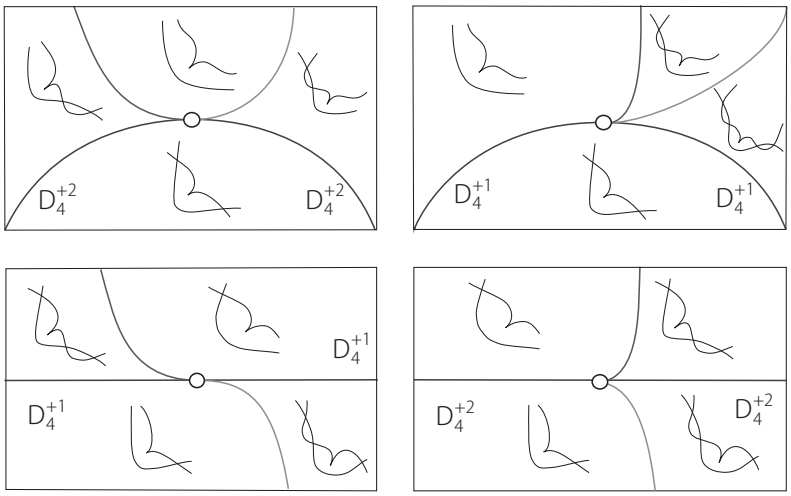

FIGURE 16. Examples of 2-parameter bifurcation of type D_4^+. Two pictures on the left (resp. right) are obtained from intersections of $\mathcal{B}_1$ (resp. $\mathcal{B}_0$) with generic surfaces containing the t-axis, see Fig.12.

[7] V.V. Goryunov, Singularities of projections of complete intersections, J. Soviet Math. 27 (1984), 2785—2811 [Translated from Itogi Nauki i Tekhniki. Ser. Sovrem. Probl. Mat. 22 (1983),167–206.]

[8] M. Hasegawa, A. Honda, K. Naokawa, M. Umehara and K. Yamada, Intrinsic invariants of cross caps, preprint, arXiv:1207.3853 (2012).

[9] Y. Kabata, Recognition of plane-to-plane map-germs, master thesis, Hokkaido University, Mar. 2014.

[10] L. Lander, The structure of the Thom-Boardman singularities of stable germs with type $\Sigma^{2,0}$, Proc. London Math. Soc. (3) 33 (1976), 113–137.

[11] R. Morris, The use of computer graphics for solving problems in singularity theory, Visualization and Mathematics, Experiments, Simulations and Environments, H. C. Hege and K. Polthier (eds.), Springer (1997), 53–66.

[12] T. Ohmoto, A geometric approach to Thom polynomials for C^∞ stable mappings, J. London Math. Soc. (2) 47 (1993), 157–166.

[13] T. Ohmoto and F. Aicardi, "First order local invariants of apparent contours" Topology, vol. 45 (2006) 27-45.

[14] R. Oset-Sinha, Topological invariants of stable maps from 3-manifolds to three-space, Dissertation, Universitat de Valencia, 2009.

[15] R. Oset-Sinha and F. Tari, Projections of surfaces in $\mathbb{R}^4$ to $\mathbb{R}^3$ and geometry of their singular images, to appear in Rev. Math. Iberoam. European Math. Soc. (2013).

[16] O. A. Platonova, Projections of smooth surfaces, J. Soviet Math. 35 no.6 (1986), 2796–2808 [Tr. Sem. I. G. Petrovskii 10 (1984), 135–149 in Russian].

[17] J. H. Rieger, Families of maps from the plane to the plane, Jour. London Math. Soc., 36 (1987), pp. 351–369.

[18] J. H. Rieger and M. A. S. Ruas, Classification of $\mathcal{A}$-simple germs from k^n to k^2 Compositio Math., 79 (1991) 99-108.

[19] K. Saji, Criteria for singularities of smooth maps from the plane into the plane and their applications, Hiroshima Math. Jour. 40 no.2 (2010), 229–239.

[20] F. Tari, On pairs of geometric foliations on a cross-cap, Tohoku Math. J. 50 (2007), 233–258.

[21] J. West, The Differential Geometry of the Cross-Cap, Dissertation, University of Liverpool (1995).

[22] T. Yoshida, Bifurcation of plane-to-plane map-germs of corank 2 and its application to robotics (in Japanese), master thesis, Hokkaido University, Mar. 2014.
[23] T. Yoshida, Y. Kabata and T. Ohmoto, Bifurcation of three parameter families of plane-to-plane map-germs, in preparation.
[24] V. M. Zakalyukin, Reconstructions of fronts and caustics depending on a parameter and versality of mappings, J. Soviet Math. 27 (1984), 2713–2735 [Translated from Itogi Nauki i Tekhniki. Ser. Sovrem. Probl. Mat. 22 (1983), 56—93.]

(T. Yoshida) Department of Mathematics, Graduate School of Science, Hokkaido University, Sapporo 060-0810, Japan
E-mail address: toshiki@mail.sci.hokudai.ac.jp

(Y. Kabata) Department of Mathematics, Graduate School of Science, Hokkaido University, Sapporo 060-0810, Japan
E-mail address: s123015@math.sci.hokudai.ac.jp

(T. Ohmoto) Department of Mathematics, Graduate School of Science, Hokkaido University, Sapporo 060-0810, Japan
E-mail address: ohmoto@math.sci.hokudai.ac.jp